MMI Multiplexer for Dual-Channel Erbium-Doped Waveguide Amplifiers

A. Bakhtazad, J. N. McMullin, C. J. Haugen and R. G. DeCorby
TRLabs, 800-10611 98 Ave Edmonton, AB CANADA T5K 2P7
bakhtaza@ee.ualberta.ca, mcmullin@edm.trlabs.ca, chaugen@edm.trlabs.ca, rdecorby@edm.trlabs.ca

Abstract: A multimode interference coupler is proposed for pumping two erbium-doped waveguide amplifiers from a single 980 nm pump channel. Simulations predict that a device less than 2500 μm long can be made with signal and pump power losses of 0.28 dB and 0.63 dB respectively. The calculated 1 dB excess loss bandwidth of the device is 57 nm.

OCIS Codes: (230.3120) Integrated optics devices, (230.7390) Waveguides, planar, (250.4480) Optical amplifiers.

References and Links

1. R. N. Ghosh, J. Shmulovich, C. F. Kane, M.R.X. deBarros, G. Nykolak, A. J. Bruce, and P. C. Becker, "8-mW threshold Er^{3+}-doped planar waveguide amplifier," IEEE Phot. Tech. Lett. **8**, 518-520 (1996).
2. K. Hattori, T. Kitagawa, M. Oguma, Y. Ohmori, and M. Horiguchi, "Erbium-doped silica-based waveguide amplifier integrated with a 980/1530 nm WDM coupler," Electron. Lett. **30**, 856-857 (1994).
3. Teem Photonics, www.teemphotonics.com.
4. T. Kitagawa, K. Hattori, Y. Hibino, Y. Ohmori, and M. Horiguchi, "Laser oscillation in Er-doped silica-based planar ring resonator," Proc. 18 th Eur. Conf. Opt. Com., 907-910 (1992).
5. F. Rottmann, A. Neyer, W. Mevenkamp, and E. Voges, "Integrated optic wavelength multiplexers on Lithium Niobate based on two-mode interference," J. Lightwave Tech. **6**, 946-952 (1988).
6. G. Zhang, S. Honkanen, A. Tervonen, C. M. Wu, and I. Najafi, "Glass integrated optics circuits for 1.48/1.55 and 1.33/1.55 μm wavelength division multiplexing and 1/8 splitting," Appl. Opt. **33**, 3371-3374 (1994).
7. T. Negami, H. Haga, and S. Yamamotto, "Guided-wave optical wavelength demultiplexer using an asymmetric Y junction," Appl. Phys. Lett. **54**, 1080-1082 (1989).
8. L.B. Soldano and E.C.M. Pennings, "Optical Multi-Mode Interference Devices Based on Self-Imaging: Principles and Applications", J. of Lightwave Tech. **13**, 615-627 (1995).
9. C. F. Janz, M. R. Paiam, B. P. Keyworth, and J. N. Broughton, "Bent waveguide couplers for (de)multiplexing of broadly-separated wavelengths using two-mode interference," IEEE Phot. Tech. Lett. **7**, 1037-1039 (1995).
10. M. R. Paiam, C. F. Janz, R. I. MacDonald, and J. N. Broughton, "Compact planar 980/1550 nm wavelength multi/demultiplexer based on multimode interference," IEEE Phot. Tech. Lett. **7**, 1180-1182 (1995).
11. Clifford R. Pollock, *Fundamentals of Optoelectronics* (Irwin, 1995), Chapter 8.
12. Prometheus 4.2, Kymata Software, www.kymata.com.

1. Introduction

Integrated amplifier modules using erbium-doped silica-based planar waveguides have been described previously in the literature [1,2] and are now commercially available [3]. Typically, a wavelength-selective fiber directional coupler is used to combine light from an external pump laser with the signal before it enters the amplifier. A fully integrated optical amplifier module would include an on-chip multiplexer for mixing the pump and signal channels. However, it has been found that simple integrated directional couplers suffer from high sensitivity with respect to fabrication tolerance [4]. Furthermore, the design of integrated directional couplers is complicated by considerations of the coupling between diverging and converging waveguides. Several other approaches are possible including two-mode interference couplers implemented in diffused waveguides [5] and asymmetric Mach-Zehnder interferometers [6]; however, these methods generally result in very long devices. Integrated couplers to mix two widely separated wavelengths have been realized using composite

#34549 - $15.00 US Received June 25, 2001; Revised August 02, 2001

asymmetric Y junctions [7]. Such Y junctions employ asymmetry in the refractive index profiles and require a more complex two-mask fabrication process.

In recent years, multimode interference (MMI) couplers based on self-imaging have been extensively studied [8]. Different approaches for mixing pump and signal powers are possible using MMIs. The simplest approach would be to use a 2×1 coupler in which separate signal and pump inputs exit a common output port. However, it turns out that in order to obtain self-imaging of both wavelengths at the same output waveguide, unacceptably long devices are required. This problem can be overcome by bending the coupler to introduce a new degree of freedom in the design. A device of this type was shown to have theoretical insertion losses of about 0.7 dB and 2dB for pump (λ = 850 nm) and signal (λ = 1550 nm) respectively [9]. MMI couplers can also perform dual channel wavelength multiplexing if one channel is in the bar-coupled state and the other is cross-coupled. One attempt to pump a signal at 1550 nm with light at 980nm has attained insertion losses at both wavelengths of approximately 0.5 dB [10].

In this paper, a novel MMI device is described which can simultaneously couple light from a single 980 nm pump into two 1550 nm optical amplifiers. The basic idea is to superimpose a symmetric 1×2 MMI splitter at 980 nm with a cross-state 2×2 MMI coupler at 1550 nm. The couplers necessarily have the same width but different lengths are required for efficient coupling of the two wavelengths into the output waveguides. This can be achieved by exploiting the fact that an MMI coupler has areas of low field intensity near the input and output waveguides where the fields are highly concentrated. This is described in greater detail in the next section. Using analytical and numerical techniques, a device less than 2500 μm long with 0.28 dB and 0.63 dB insertion loss for pump and signal respectively is demonstrated. Over a 57 nm band, the excess loss deviates less than 1 dB.

2. Two-Wavelength MMI Splitter/Coupler: Concept

Fig. 1 shows the calculated electric field intensity near the input of a center-fed 1×2 symmetric MMI coupler. On either side of the waveguide/MMI interface are triangular shadow regions in which the intensity of the field is very small.

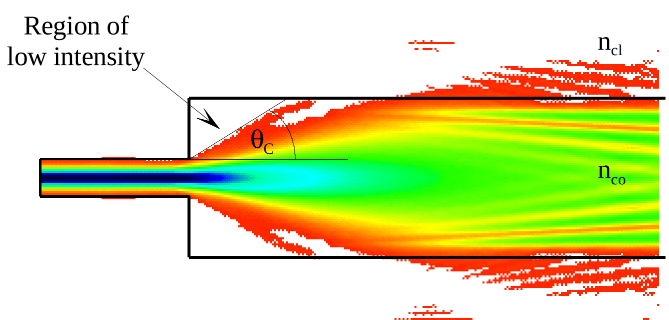

Fig.1 Field pattern near the input of a center-fed MMI coupler. Input waveguides for a signal of different wavelength can be introduced into a dead zone without disrupting the original field.

By extending the input waveguides for a different wavelength into the shadow regions on either side of the central input, it is possible to combine a symmetric center-fed 1×2 980 nm pump MMI of length L' with a 2×2 cross-state MMI of the same width, W, but different length, L, carrying two 1550 nm signal channels. Thus the MMI has three input waveguides and two output waveguides as shown in Fig. 2(a). The intruding signal waveguides have a negligible effect on the performance of the pump MMI as long as the taper boundaries are outside the limits of the diverging pump field.

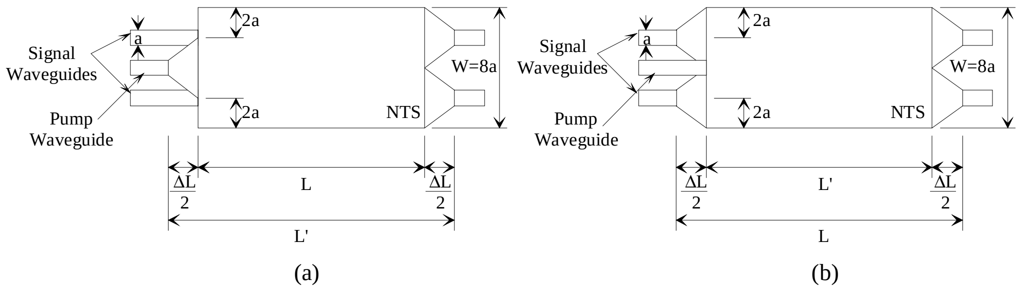

Fig. 2 (a) Proposed structure if $L < L'$. (b) Proposed structure if $L > L'$. Note that the diagrams are not shown to scale.

The assumed geometies of the two structures considered in this paper are shown in the Fig. 2(a) and 2(b). In these structures, the waveguides have a width a and the central body of the MMI device has a width of 8a. In 2(a), the untapered inputs of the 2×2 signal coupler are placed at $W/4$ = 2a from the sides of the MMI in the shadow regions and the pump MMI is longer by ΔL than the signal MMI. By adjusting the 2×2 MMI length, L, and therefore the position of the output image with respect to the output tapers, the output coupling loss of signal channels can be minimized. In Fig. 2(b), the reverse is true and the MMI length is adjusted to minimize the output coupling loss of the pump. In both cases, the length difference, ΔL, is divided evenly between input and output tapers and the end of the shorter MMI is taken to be at the start of the output tapers. Although this puts the theoretical self-imaging planes of the two couplers at different places, in practice this is of no consequence since the taper length is very much shorter than the overall MMI length. Tapering of the output waveguides is not required but it can be used to improve the output coupling of the signal channels as shown below in the detailed design case.

The longest taper length $\Delta L/2$ that can be used without severely disrupting the input field can be estimated from ray theory. The maximum angle from the input waveguide axis for rays entering the MMI from the waveguide is (see Fig. 1)

$$\theta_c = \cos^{-1} \frac{n_{cl}}{n_{co}} \tag{1}$$

where n_{cl} and n_{co} are the effective refractive indices of cladding and core respectively at the wavelength of interest. The intruding waveguide, $\Delta L/2$ longer and separated by W/4 = 2a, will not intersect this outermost ray as long as the following condition is satisfied:

$$\frac{\Delta L/2}{W/4} \leq \cot(\theta_c)\,. \tag{2}$$

This restriction on ΔL is easier to satisfy when a soft boundary is used. That is, when there is only a small difference between n_{cl} and n_{co}, θ_c is smaller and ΔL could be larger which is advantageous when trying to optimize the MMI design for two different widely separated wavelengths.

3. Two-Wavelength MMI Splitter/Coupler: Optimized Design Example

Next, the procedure used to find an optimized design based on one of the two structures of Fig. 2 is outlined. A SiON/SiO$_2$ material system with n_{SiON} = 1.565 (1.561) and n_{SiO_2} = 1.465 (1.460) at the pump (signal) wavelength is assumed. The pump and signal waveguides are taken to be ridge waveguides of width a = 3μm with cross-sections as depicted in Fig. 3. Calculations show that these waveguides support only one vertical mode at 1550 nm and two vertical modes at 980 nm. Using the simple effective index method [11] to reduce this 3D

#34549 - $15.00 US
Received June 25, 2001; Revised August 02, 2001

structure to an equivalent 2D one, the corresponding fundamental vertical effective indices are found to be:

$$n_{\mathrm{co}} = 1.5213 \text{ and } n_{\mathrm{cl}} = 1.4592 \text{ at } \lambda_{1,2} = 1550\,\mathrm{nm}\,, \tag{3a}$$

$$n'_{\mathrm{co}} = 1.5471 \text{ and } n'_{\mathrm{cl}} = 1.4859 \text{ at } \lambda_0 = 980\,\mathrm{nm}\,. \tag{3b}$$

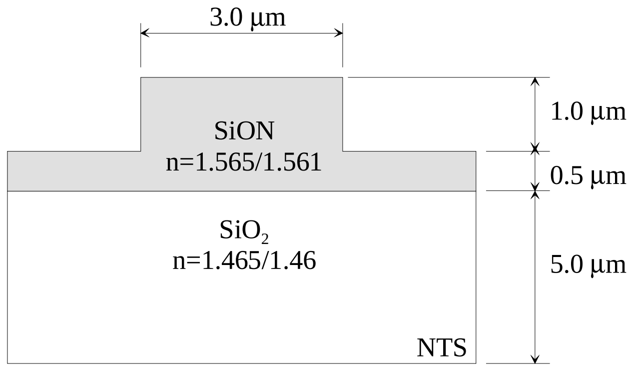

Fig. 3 Silica-based glass waveguide system. The shown values of refractive indices are for 980/1550 nm respectively.

The width of the MMI structure is taken to be W = 8a = 24 µm. Assuming that the difference between real and effective width of the MMI coupler is of second order in importance, the length, L, of the 2×2 cross-state MMI for the two 1550 nm channels is approximately [8]

$$L \approx 3L_\pi \tag{4}$$

where $L_\pi = \pi/(\beta_0 - \beta_1)$ is the beat length for an ideal MMI coupler at the signal wavelength, and β_0 and β_1 are the propagation constants of the fundamental and first modes. The assumed waveguide parameters result in L_π = 827.4 µm and L = 2482 µm. For a symmetric MMI splitter at 980 nm, the device lengths for two-fold images are

$$L' \approx \frac{p}{2} \times \frac{3}{4} L'_\pi = \frac{p}{2} \times \frac{3}{4}(1286.6\mu\mathrm{m}) = p(482.5)\ \mu\mathrm{m}\,,\ p = 1,2,3,\ldots \tag{5}$$

As a first step, p is chosen to make L and L' as near to each other as possible. It is found that taking p = 5, L' = 2412, minimizes the difference and therefore

$$\Delta L = L - L' \approx 2482 - 2412 = 70\ \ \mu\mathrm{m}\,. \tag{6}$$

Hence, the 1×2 symmetrical MMI splitter is shorter than the cross-state 2×2 MMI coupler and the structure of Fig. 2(b) should be used.

To check the validity of these calculations, numerical simulations of the 1×2 and 2×2 MMIs were carried out using a commercial beam propagation package [12]. An optimum length L' = 2394 µm of the 1×2 symmetric MMI structure was obtained which is close to the estimated value of L' = 2412 µm and the coupling loss was found to be 0.73 dB. Similarly, the optimum length of 2×2 MMI coupler is L = 2463 µm so that ΔL = 69 µm. The coupling loss is 1.45 dB and the cross-talk is –19.43 dB.

Next, simulations of the composite structure of Fig. 2(b) were carried out. At 980 nm, the loss increased to 1.48 dB while the coupling loss at 1550nm decreased to 0.67 dB and the cross-talk was –26.54 dB. Note that the difference length of 69 µm does not satisfy the condition of Eq. (2) at 980 nm. For that wavelength, $n_{\mathrm{cl}}/n_{\mathrm{co}}$ = 0.9604 (see Eq. 3(b)) and ΔL_{max} = 41.4 µm leading to an increase in the 980 nm coupling loss of 0.75 dB; however, the coupling loss at 1550 nm is decreased by 0.68 dB

#34549 - $15.00 US Received June 25, 2001; Revised August 02, 2001

Assuming that tapering can increase the performance of the 2×2 MMI structure, an attempt was made to change the design lengths in order to decrease the signal coupling loss while keeping the loss of pump power as small as possible. For the structure shown in Figure 2(b), ΔL was varied and a length L' that minimizes the loss at 1550 nm was found. Similarly, the length L' that minimizes the loss at 980 nm was found. Fig. 4 shows the device lengths at 1550 nm and 980 nm as a function of the tapering length $\Delta L/2$ along with their corresponding insertion loss. Compromising for low loss at both wavelengths, ΔL is chosen at the point where the difference between the 980 nm and 1550 nm device lengths is minimized. The optimum device length is then chosen to be the length that minimizes the loss at 1550 nm. Referring to Fig. 4, we obtain

$$\Delta L_{\text{optim}}/2 = 42\,\mu\text{m}\text{ , and } L'_{\text{optim}} = 2364\,\mu\text{m}\text{ .}$$

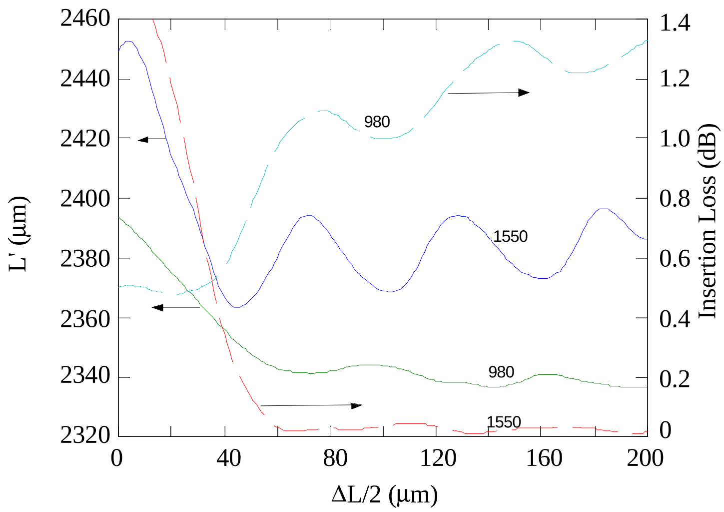

Fig 4 Optimum device length at 1550 nm and 980 nm versus tapering length. The corresponding insertion loss as a function of tapering length is also shown

With this design, the coupling loss of the pump is reduced to 0.63 dB (0.85 decrease) and, more importantly, the coupling loss of the signal power is only 0.28 dB (0.39 dB decrease). The cross-talk is also reduced to –44.9 dB.

The field patterns of the optimized device when operating at 1550 nm and 980 nm are plotted in Figs. 5(a) and 5(b) respectively. It is apparent from the oscillation of the field pattern in the output waveguides in Fig. 5(b) that a portion of the input pump power has been converted to the second order mode.

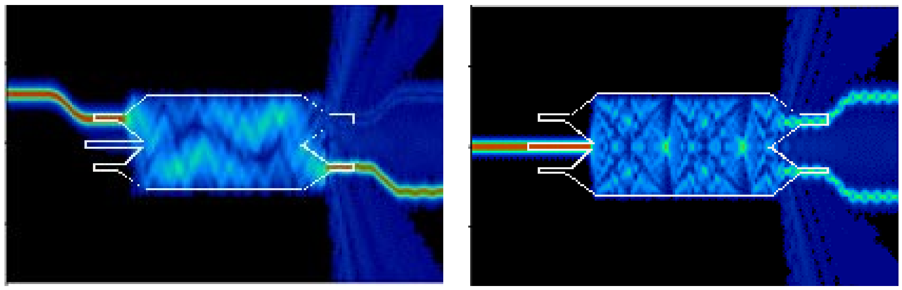

(a) (b)

Fig 5 (a) The field pattern of the optimized device for one 1550 nm signal. (b) The field pattern of the optimized device for the 980 nm pump signal.

In Figure 6, the frequency response of the device is shown along with the results of an analysis of the sensitivity of the device to variations in length and width. Between 1524 nm and 1581 nm, the insertion loss of the signal varies by less than 1 dB. The sensitivity analysis reveals that the device is much less tolerant to changes in width than changes in length. A change in width of only 0.2 μm (0.008 *W*) results in an extra loss of 1 dB while the same effect is only achieved with a variation in length of 36 μm (0.01 *L*). This tolerance to changes in length may be partly due to implementing tapering in the input and output ports.

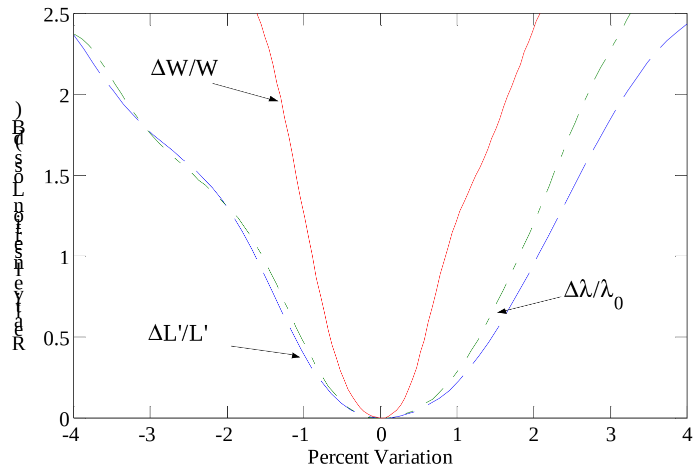

Fig. 6 Sensitivity of excess loss to variations in wavelength, MMI width and MMI length.

4. Conclusion

A new approach to wavelength selective couplers for erbium-doped waveguide amplifiers has been described. Using dead zones in the field intensities, it is shown that a single structure can be designed to operate as a multimode interference coupler for both pump and signal wavelengths. At the pump wavelength, the device evenly distributes the pump power into two output waveguides. At the signal wavelength, the device directs two inputs to the two separate outputs with low cross-talk. Including tapering of the coupling waveguides as part of the MMI structure, an optimum structure can be found by minimizing the signal power insertion loss while maintaining the pump power loss as low as possible. Detailed simulations of a silicon oxynitride system with ridge waveguides 3 μm wide, shows that the total device length is below 2.5 mm, and pump and signal power losses are theoretically 0.28 dB and 0.63 dB respectively and the signal cross-talk is –44.9 dB. The 1 dB bandwidth of the device, centered at 1550nm, is relatively wide at 57 nm. Another attractive feature of this device is that it can be fabricated with a single lithography step.

Acknowledgements

The authors would like to thanks TR*Labs* for providing the research facilities and financial support necessary to complete this work.